



HAL
open science

Mathematical study of feedback control roles and relevance in stress erythropoiesis

Fabien Crauste, Ivan Demin, Olivier Gandrillon, Vitaly Volpert

► **To cite this version:**

Fabien Crauste, Ivan Demin, Olivier Gandrillon, Vitaly Volpert. Mathematical study of feedback control roles and relevance in stress erythropoiesis. *Journal of Theoretical Biology*, 2010, 263 (3), pp.303. 10.1016/j.jtbi.2009.12.026 . hal-00567288

HAL Id: hal-00567288

<https://hal.science/hal-00567288>

Submitted on 20 Feb 2011

HAL is a multi-disciplinary open access archive for the deposit and dissemination of scientific research documents, whether they are published or not. The documents may come from teaching and research institutions in France or abroad, or from public or private research centers.

L'archive ouverte pluridisciplinaire **HAL**, est destinée au dépôt et à la diffusion de documents scientifiques de niveau recherche, publiés ou non, émanant des établissements d'enseignement et de recherche français ou étrangers, des laboratoires publics ou privés.

Author's Accepted Manuscript

Mathematical study of feedback control roles and relevance in stress erythropoiesis

Fabien Crauste, Ivan Demin, Olivier Gandrillon, Vitaly Volpert

PII: S0022-5193(09)00599-2
DOI: doi:10.1016/j.jtbi.2009.12.026
Reference: YJTBI5816



www.elsevier.com/locate/jtbi

To appear in: *Journal of Theoretical Biology*

Received date: 30 June 2009
Revised date: 26 November 2009
Accepted date: 23 December 2009

Cite this article as: Fabien Crauste, Ivan Demin, Olivier Gandrillon and Vitaly Volpert, Mathematical study of feedback control roles and relevance in stress erythropoiesis, *Journal of Theoretical Biology*, doi:[10.1016/j.jtbi.2009.12.026](https://doi.org/10.1016/j.jtbi.2009.12.026)

This is a PDF file of an unedited manuscript that has been accepted for publication. As a service to our customers we are providing this early version of the manuscript. The manuscript will undergo copyediting, typesetting, and review of the resulting galley proof before it is published in its final citable form. Please note that during the production process errors may be discovered which could affect the content, and all legal disclaimers that apply to the journal pertain.

Mathematical study of feedback control roles and relevance in stress erythropoiesis

Fabien Crauste^a, Ivan Demin^{*,a}, Olivier Gandrillon^b, Vitaly Volpert^a

^aUniversité de Lyon, Université Lyon 1,
CNRS, UMR 5208, Institut Camille Jordan,
Batiment du Doyen Jean Braconnier,
43, blvd du 11 novembre 1918,
F - 69222 Villeurbanne Cedex, France

^bEquipe "Bases Moléculaires de l'Autorenouvellement et de ses Altérations"
Université de Lyon, Lyon, F-69003, France ;
Université Lyon 1, Lyon, F-69003, France ;
CNRS, UMR5534, Centre de génétique moléculaire et cellulaire,
Villeurbanne, F-69622, France

Abstract

This work is devoted to mathematical modelling of erythropoiesis. We propose a new multi-scale model, in which we bring together erythroid progenitor dynamics and intracellular regulatory network that determines erythroid cell fate. All erythroid progenitors are divided into several sub-populations according to their maturity. Two intracellular proteins, Erk and Fas, are supposed to be determinant for regulation of self-renewal, differentiation and apoptosis. We consider two growth factors, erythropoietin and glucocorticoids, and describe their dynamics. Several feedback controls are introduced in the model. We carry out computer simulations of anaemia and compare the obtained results with available experimental data on induced anaemia in mice. The main objective of this work is to evaluate the roles of the feedback controls in order to provide more insights into the regulation of erythropoiesis. Feedback by Epo on apoptosis is shown to be determinant in the early stages of the response to anaemia, whereas regulation through intracellular regulatory network, based on Erk and Fas, appears to operate on a long-term scale.

Key words: Anaemia, Intracellular Regulatory Network, Growth Factor, Bistability

*Corresponding author. Tel: +33 472 432 765. Fax: +33 472 431 687.

Email addresses: crauste@math.univ-lyon1.fr (Fabien Crauste),
demin@math.univ-lyon1.fr (Ivan Demin), gandrillon@cgm.c.univ-lyon1.fr (Olivier Gandrillon), volpert@math.univ-lyon1.fr (Vitaly Volpert)

1. Introduction

All blood cells can be divided into three categories, red blood cells, white blood cells and platelets. Red blood cells (RBCs) are produced during a complex process called erythropoiesis, which is a part of haematopoiesis (production of blood). It involves haematopoietic stem cells, at the root of blood cell production, able to create all haematopoietic lineages [41], first lymphoid and myeloid lineages, then, within the myeloid branch, different lineages and in particular erythroid lineage, the origin of red blood cells. Haematopoietic stem cells differentiate into immature erythroid cells, called erythroid progenitors, which are undifferentiated cells committed to erythroid lineage. Then, through maturation and differentiation stages, erythroid progenitors become reticulocytes, which are almost mature red blood cells. These latter end their maturation to become red blood cells and enter blood stream, where they transport oxygen to tissues.

Erythropoiesis consists in a series of cell divisions through which erythroid cells acquire differentiation markers. This process allows the production of sufficient amount of erythrocytes to transport oxygen to organs. Erythropoiesis can sometimes exhibit disorders, such as excessive proliferation of immature cells, as observed in acute leukaemias [21, 28]. Such disorders can be caused by alteration of intracellular regulatory networks, which control cell fate (e.g. Madan et al. [26]), that is self-renewal (the ability to produce daughter cells of the same maturity), differentiation (the ability to produce more mature daughter cells) or apoptosis (programmed cell death). By maturity here we understand an accumulation of differentiation markers (like haemoglobin, for example). Hence, the regulation of erythropoiesis depends on a precise control of cell fate by means of intracellular proteins and growth factors.

One of the most studied growth factors, playing an important role in erythropoiesis regulation, is erythropoietin (Epo), a glucoprotein released by the kidney in response to hypoxia, that is a lack of oxygen in tissues. Glucocorticoids (GCs) are lipophilic hormones involved in the regulation of various physiological responses, and in particular in stress erythropoiesis. They are known to favour cell proliferation [22]. Growth factors operate by activating membrane receptors on cell surface to trigger intracellular protein activation.

Recently, Rubiolo et al. [34] proposed a description of the regulatory network that controls erythroid progenitor fate: some proteins are involved in a self-renewal loop, others in a differentiation/apoptosis loop, see Figure 1. The first loop self-activates and inhibits the second one, whereas the second loop can inhibit the first one and, depending on Epo levels, induce either erythroid progenitor differentiation or apoptosis. Self-renewal loop relies on proteins of the MAPK family, the other loop is mainly controlled by Fas, a protein of the tumour-necrosis factor family.

Pioneering models of erythropoiesis regulation were proposed by Wichmann and Loeffler [42], who modelled the dynamics of haematopoietic stem cells, erythroid progenitors and erythroid precursors (reticulocytes). They considered feedback controls from reticulocytes on progenitors and from progenitors on

stem cells, they confronted their models with experimental data on stress erythropoiesis (bleeding, irradiation) and fitted model parameters. Later Wulff et al. [44] and Wichmann et al. [43] improved Wichmann and Loeffler's models. Bélair et al. [7] proposed a model of erythropoiesis, partially based on previous works by Mackey [23, 24] and Mackey and Rudnicki [25] on haematopoietic stem cell dynamics. In Bélair et al. [7] the authors proposed an age-structured model describing erythroid cell dynamics, including an explicit control of differentiation by erythropoietin. This model was then improved by Mahaffy et al. [27]. Other works inspired by Bélair et al. [7] proposed mathematical models of erythropoiesis [1, 2, 5]. The erythropoietin-mediated inhibition of apoptosis has been considered in Adimy and Crauste [3]. The authors focused on the appearance of periodic haematological diseases, such as periodic chronic myeloid leukaemia [16]. Recently we proposed an age-structured model of erythropoiesis taking into account feedback controls on progenitor self-renewal and apoptosis [11]. We confronted the model with experimental data on anaemia induced by phenylhydrazine injections and concluded the relevance of erythroid progenitor self-renewal for the response to stress.

Modelling of regulatory networks, involved in cell decision, has been the subject of recent analysis of lineage specification. Erythrocytes and platelets have one myeloid progenitor in common, known as megakaryocytic-erythroid progenitor (MEP). As a result of competition between two proteins, PU.1 and GATA-1, the MEP differentiates either into an erythroid progenitor or into a megakaryocytic progenitor. This choice has been studied by Roeder and Glauche [33] and Huang et al. [19]. In both studies, models proposed by the authors demonstrated a bistable behaviour. This idea has been further developed in Chickarmane et al. [10].

The main objective of this work is to develop a model of erythropoiesis which would allow evaluating the roles of different feedback controls in regulation of erythropoiesis in stress situations. We bring together interactions at the cell population level, growth factor actions and regulation of cell fate by intracellular proteins. From Rubiolo et al. [34] we identify key proteins involved in the regulation of self-renewal, differentiation and apoptosis, and describe interactions between them. The resulting system is coupled with a model of erythroid cell dynamics. This latter, inspired by Demin et al. [14], describes cell dynamics using self-renewal, differentiation and apoptosis rates of erythroid progenitors. The rates are determined by intracellular proteins, whereas growth factors and reticulocyte count control evolution of the intracellular proteins. Erythrocyte count, in turn, is responsible for growth factor production. The resulting model is confronted with experimental data on a severe anaemia, which allows determining the roles of the different feedback controls and their relative influences on regulation of stress erythropoiesis. We introduce the following feedback controls: in stress situations Epo inhibits apoptosis independently of intracellular regulatory network based on Erk and Fas [18, 36], Epo and GCs promote Erk activation [34, 37], reticulocytes upregulate Fas [13].

The work is organised as follows. In Section 2, we describe intracellular regulatory mechanisms, using available biological information. The resulting

model is a nonlinear system of ordinary differential equations. This system describes the dynamics of two key proteins for cell fate regulation, Erk and Fas. We investigate the bistable behaviour of this system in order to explain the choice between cell self-renewal and differentiation or apoptosis. In Section 3 we present erythroid progenitor dynamics and dynamics of growth factors. We consider several sub-populations of erythroid cells according to their maturity. Two main growth factors involved in erythropoiesis regulation are considered: Epo and GCs. We obtain the complete model in Section 4. This multi-scale model is composed with $3(n+1)$ equations, where n is the number of erythroid progenitor sub-populations. Existence of steady states and their stability are briefly discussed in Section 4.2. In Section 6 we present simulations of anaemia and investigate the roles of different feedback functions for the regulation of erythropoiesis. The simulations are confronted with experimental data on anaemia, induced by injection of phenylhydrazine [9]. Roles of feedback controls by Epo on apoptosis rate, independently of the considered intracellular network, and by the intracellular regulatory network on cell fate are evaluated. Results show that both controls are important for the response, yet they do not operate at the same time and appear to have specific roles. We conclude with a discussion and present possible research directions indicated by this model.

2. Intracellular regulatory network

In a recent paper Rubiolo et al. [34] investigated the differentiation process of erythroid progenitors. In particular, they identified key proteins involved in self-renewal and differentiation/apoptosis, see Figure 1. Differentiation and apopto-

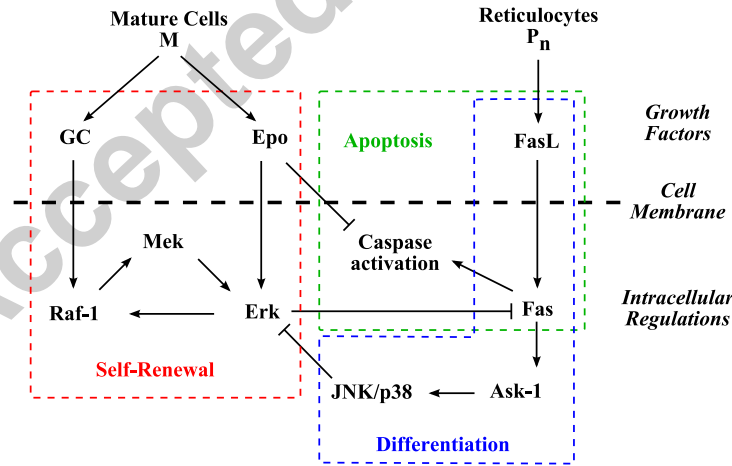


Figure 1: Summary of intracellular protein interactions that determine erythroid progenitor fate, partially adapted from Rubiolo et al. [34].

sis appear to be controlled by the same proteins. In fact, different proteins are

involved both in cell differentiation and cell apoptosis, however, depending on external conditions, cells undergo either differentiation or apoptosis. For example, Epo has been shown to inhibit erythroid progenitor apoptosis [20]. Hence, when Epo levels are low, erythroid progenitors preferentially die by apoptosis, whereas with high Epo levels they differentiate.

Rubiolo et al. [34] showed that self-renewal was controlled by the self-activated cascade Raf-1 - Mek - Erk, whereas differentiation was controlled by the cascade Fas - Ask-1 - Jnk/p38, Fas triggering also cell apoptosis. This latter protein cascade is inhibited by the former, and vice versa. Hence, erythroid progenitor self-renewal and differentiation/apoptosis processes are controlled by two inhibitor loops, one being self-activating. Two proteins are of particular interest: Erk and Fas. The former is the cornerstone of the inhibition of differentiation and apoptosis. Erk (Extracellular signal-Regulated Kinase) is a member of the MAPK family, also known as the classical MAP kinase, it regulates cell proliferation and differentiation. Fas belongs to the tumour necrosis factor family (TNF), it induces cell apoptosis. We focus our attention on the interaction between these two proteins, that are key regulators of erythroid progenitor fate.

As mentioned in Figure 1, external signals activate intracellular proteins. Epo is known to have the dual action of being both a mitogen and a survival factor [36]. The molecular mechanisms involved have been clarified (for a review, see Sawyer and Jacobs-Helber [35]): Epo prevents apoptosis of erythroid progenitors through Stat5/GATA-1/Bcl-xL pathway [18], that is largely independent of the Erk pathway [8, 30, 38]. Self-renewal promoting activity of Epo, on the contrary, seems to rely mainly on the activation of the Erk kinase [34, 37]. We therefore decided to integrate separately these two aspects of Epo action in the model: prevention of apoptosis is modelled as a direct mechanism, i.e. the molecular players are not explicitly taken into account. This feedback is assumed to be independent of the intracellular regulatory network based on Erk and Fas interactions. This is introduced in Section 4.1, Equation (12). On the contrary, self-renewal is modelled as an Erk-dependent mechanism, which is introduced below in this section. GCs are involved in regulation of stress erythropoiesis [6, 17]. They activate self-renewing loop by increasing the level of Raf-1 expression.

One source term of activation appears in Figure 1 concerning the differentiation/apoptosis part. Fas-ligand, denoted by FasL, a membrane protein, activates the transmembrane protein Fas. De Maria et al. [13] suggested the existence of a negative regulatory feedback between mature and immature erythroid progenitors, in which mature cells exert a cytotoxic effect on immature cells. Mature erythroid progenitors, called reticulocytes, express FasL, which stimulates activation of Fas in immature erythroid progenitors. Sensitivity to FasL decreases with cell maturation. Other external factors, such as c-Kit, the protein associated with the stem cell factor (SCF) [29], proteins from the JAK family [39], etc., regulate the levels of activated intracellular proteins. Yet, we cannot take all these proteins into account, and we focus, in the following, on Epo, GCs, and FasL.

Focusing on Erk and Fas and interactions between them, we will state a

system of ODEs, which represents the intracellular regulatory network shown in Figure 1. Denote by E and F the expressions of Erk and Fas respectively. The following system describes how they evolve in time,

$$\begin{cases} \frac{dE}{dt} = (\alpha + \beta E^k)(E_0 - E) - aE - bEF, \\ \frac{dF}{dt} = \gamma(F_0 - F) - cEF - dF. \end{cases} \quad (1)$$

Let us explain how this system is obtained. Consider first activation of Erk and Fas. As discussed above, Erk activation is due to Epo. From the scheme we can see that GCs also activate Erk through kinase cascade Raf-1 - Mek - Erk. This activation is described by term $\alpha = \alpha(Epo, GC)$. Moreover, Erk self-activates, which is described by term βE^k with some positive constant $k > 0$. When more Erk is activated, less Erk receptors remain free and, thus, activation rate saturates. This gives the following overall term for Erk activation, $(\alpha + \beta E^k)(E_0 - E)$ with threshold value of Erk expression E_0 , which cannot be overpassed. In similar way we describe FasL related activation of Fas by term $\gamma(FasL)(F_0 - F)$. Fas inhibits Erk through Fas - Ask1 - JNK/p38 kinase cascade. The rate of the inhibition is thus proportional to Erk and Fas. We describe this inhibition by term $-bEF$ in equation for Erk (by term $-cEF$ in equation for Fas since the inhibition process consumes Fas). Finally, we add an elimination term for both Erk and Fas, and obtain System (1), that describes the intracellular regulatory network shown in Figure 1. It should be noted that this system is well-posed in the sense that Erk and Fas expressions cannot become negative and are bounded.

To find steady states of System (1), we must solve

$$\frac{dE}{dt} = 0 \quad \text{and} \quad \frac{dF}{dt} = 0,$$

that is

$$F = \frac{(\alpha + \beta E^k)(E_0 - E)}{bE} - \frac{a}{b} \quad \text{and} \quad F = \frac{\gamma F_0}{cE + d + \gamma}. \quad (2)$$

Depending on the parameter values, (2) can have one to three solutions. Indeed, denote by ξ and χ the following functions,

$$\xi(E) = \frac{(\alpha + \beta E^k)(E_0 - E)}{bE} - \frac{a}{b} \quad \text{and} \quad \chi(E) = \frac{\gamma F_0}{cE + d + \gamma}. \quad (3)$$

Then one easily obtains that χ is a bounded positive decreasing function, mapping the interval $[0, E_0]$ into $[\gamma F_0/(cE_0 + d + \gamma), \gamma F_0/(d + \gamma)]$. The function ξ satisfies

$$\lim_{E \rightarrow 0} \xi(E) = +\infty \quad \text{and} \quad \xi(E_0) = -\frac{a}{b} < 0.$$

Consequently, System (1) has at least one steady state.

The analysis of the variations of function ξ , easy though tedious, shows that for some values of the parameters ξ is decreasing, hence System (1) has only one steady state. For other parameter values however, ξ is not monotonous and up to three steady states may exist. In particular, to obtain existence of three steady states it is necessary that $k > 1$.

The case of three steady states is shown in Figure 2. The points A and C are stable nodes, the point B is a saddle. The point A corresponds to high levels of activated Fas and low levels of activated Erk, whereas the point C corresponds to low levels of activated Fas and high levels of activated Erk. Hence, the point A is associated with erythroid progenitor differentiation or apoptosis, the point C with erythroid progenitor self-renewal.

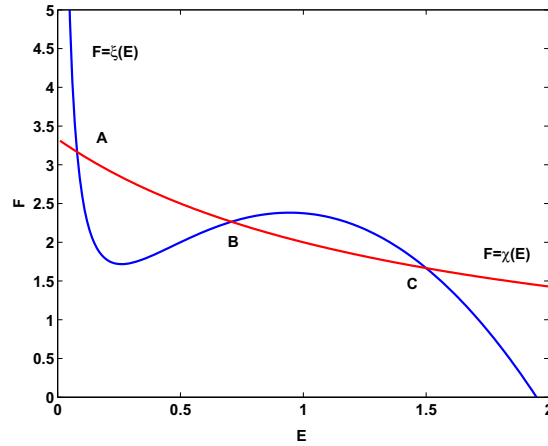


Figure 2: Curves defined by (3). Three intersection points determine steady states of System (1). Two of them, A and C , are stable. Parameters used are given in Section 5.2 when dealing with numerical simulations of the complete multi-scale model.

If α and γ are not constant but dynamically depend on growth factors, then, during a response to a stress, values of α and γ can be such that temporarily the number of steady states of System (1) goes from three to only one, and all cells, then, undergo either self-renewal or differentiation/apoptosis.

In the next section we discuss erythroid progenitor dynamics. The resulting model is coupled to System (1) in Section 4.

3. Erythroid Progenitor Dynamics

Since erythroid cell sensitivity to external signals strongly depends on the maturity, we consider several erythroid progenitor differentiation stages, called sub-populations, characterised by their maturity. We suppose there are n erythroid progenitor sub-populations, with $n > 1$ fixed. Let us denote by P_i , $i = 1, \dots, n$, the number of progenitors in the i -th sub-population per μl of

blood, and by s_i , d_i and a_i their rates of self-renewal, differentiation and apoptosis, respectively. For the sake of simplicity we consider only symmetric cell division. Considering asymmetric cell division would modify expressions for self-renewal and differentiation rates but the model would remain similar. Then, progenitor self-renewal produces two daughter cells with the same maturity as the mother cell, thus, the two cells belong to the same sub-population. Differentiation produces two cells, which are more mature, and then belong to the next sub-population, see Figure 3. Dynamics of erythroid progenitors are described

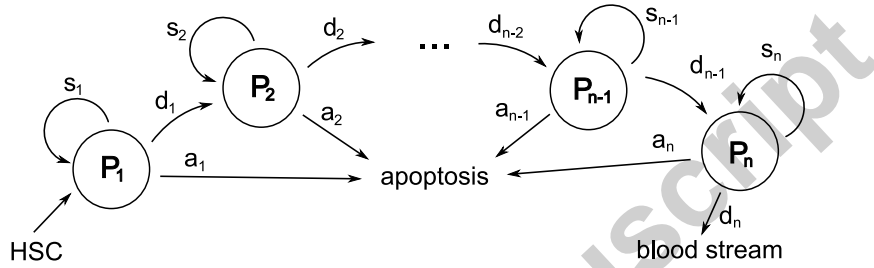


Figure 3: Differentiation scheme of erythroid progenitors. P_i , $i = 1, \dots, n$, denotes the number of progenitors in the i -th sub-population per μl of blood, and by s_i , d_i and a_i their rates of self-renewal, differentiation and apoptosis, respectively.

by the following system of differential equations [14],

$$\frac{dP_1}{dt} = HSC + s_1 P_1 - d_1 P_1 - a_1 P_1, \quad (4)$$

where HSC accounts for the cell influx from the stem cell compartment, and for $i = 2, \dots, n$,

$$\frac{dP_i}{dt} = 2d_{i-1} P_{i-1} + s_i P_i - d_i P_i - a_i P_i. \quad (5)$$

Moreover, we denote by M the number of erythrocytes per μl of blood, which satisfies

$$\frac{dM}{dt} = d_n P_n - \delta M, \quad (6)$$

where δ is the natural mortality rate of erythrocytes.

The term red blood cell (RBC) refers to an erythroid cell which circulates in the blood flow and carries oxygen to tissues. It can be an erythrocyte or a reticulocyte. During normal erythropoiesis very few reticulocytes circulate in the blood. For this reason and since we do not consider spatial aspects of erythropoiesis that could allow distinguishing between circulating reticulocytes and reticulocytes in the bone marrow, we assume that RBC count equals erythrocyte count. RBC count is determinant for the release of various growth factors in the blood stream. For instance, due to a lack of oxygen, kidneys release Epo. RBCs also induce the release of glucocorticoids in stress situations [6].

Denote by Epo and GC the blood levels of erythropoietin and glucocorticoids respectively. They are supposed to satisfy ordinary differential equations [7, 27],

$$\frac{dEpo}{dt} = f_{Epo}(M) - k_{Epo} Epo, \quad (7)$$

$$\frac{dGC}{dt} = f_{GC}(M) - k_{GC} GC, \quad (8)$$

where k_{Epo} and k_{GC} are degradation constants, and f_{Epo} and f_{GC} are production terms. They depend on the number of erythrocytes, and are supposed to be positive, bounded, decreasing functions, since the more erythrocytes the lower erythropoietin and glucocorticoid levels.

In the next section we couple intracellular protein dynamics with cell population dynamics, and obtain a multi-scale model of erythropoiesis.

4. Model of Erythropoiesis

4.1. Coupling the two scales

To simplify the modelling, we neglect variations in cell cycle durations, so cell cycle lengths are supposed to be constant, equal to T_c . Each cell cycle ends up with either self-renewal, differentiation or apoptosis. Then, on every time unit

$$s_i + d_i + a_i = \frac{1}{T_c}.$$

Since erythroid progenitors perform one cell cycle in about 24 hours [11], and the time unit considered in this paper is also 24 hours, we suppose $T_c = 1$ and the above equality becomes

$$s_i + d_i + a_i = 1. \quad (9)$$

Let us specify how these rates are defined. This is used later in this section and in Section 5.3. Denote by p_s the probability of self-renewal provided that the cell does not undergo apoptosis. Then the probability of differentiation p_d , provided that the cell does not undergo apoptosis, is $p_d = 1 - p_s$. Since cell cycle time is fixed and equals one time unit, we can then write s and d (subscripts are deliberately omitted) as

$$s = (1 - a)p_s, \quad d = (1 - a)(1 - p_s). \quad (10)$$

The term $1 - a$ accounts for the rate of survival to apoptosis. Consequently, s denotes the overall self-renewal rate, which is in fact expressed by the probability of self-renewal of non-apoptotic cells p_s multiplied by the rate of survival $1 - a$. The same holds for the differentiation rate.

As described in Section 2, self-renewal, differentiation and apoptosis rates depend on one hand on the intracellular protein regulatory network inherent to each erythroid progenitor, and on another hand apoptosis is inhibited by Epo.

Proteins Erk and Fas have been previously identified as the main regulators of erythroid progenitor fate, see Section 2. Erk induces self-renewal, and inhibits differentiation and apoptosis, whereas Fas inhibits self-renewal and induces differentiation or apoptosis, depending on Epo blood concentration. Concentrations of Erk and Fas, denoted by E and F , satisfy System (1), where constants α and γ account for external sources of Erk and Fas activators, respectively. As mentioned in Section 2, the source of Erk activator consists mainly in erythropoietin and glucocorticoids. Hence, we assume α is an increasing function of Epo and GC ,

$$\alpha = \alpha(Epo, GC).$$

Parameter γ stands for activation of Fas by FasL, which is expressed on surface of reticulocytes. Hence, we assume γ depends on P_n , which correspond to reticulocytes, and the sensitivity of γ to P_n decreases with maturity level i , so that

$$\gamma = \gamma_i(P_n),$$

and γ_i is a positive, bounded and increasing function.

Finally, before stating the system verified by concentrations E and F , let us present the last assumption. As explained in the previous section, quantities of Erk and Fas are supposed to have maximum values, denoted by E_0 and F_0 respectively. Usually, exact quantities of Erk and Fas in erythroid cells cannot be measured, rather relative levels of activated Erk and Fas are provided. Hence, in order to render this model more comprehensible, we normalise activated Erk and Fas quantities, denoting by E and F the ratios E/E_0 and F/F_0 . This guarantees the variables E and F to be between 0 and 1. Thus, E_i and F_i , the levels of activated Erk and Fas in the i -th progenitor sub-populations, satisfy the following system, obtained from (1),

$$\begin{cases} \frac{dE_i}{dt} = (\alpha(Epo, GC) + \beta E_i^k) (1 - E_i) - aE_i - bE_i F_i, \\ \frac{dF_i}{dt} = \gamma_i(P_n)(1 - F_i) - cE_i F_i - dF_i, \end{cases} \quad (11)$$

where β , a , b , c and d respectively stand for βE_0^k , aE_0 , $bE_0 F_0$, $cE_0 F_0$ and dF_0 . Note that all cells of a sub-population are assumed to express the same levels of activated Erk and Fas. This is a strong hypothesis, because in reality, different progenitors with the same maturity express different levels of Erk and Fas indicating stochasticity in protein expression. This stochasticity certainly plays an important role in erythropoiesis, yet in this model we do not take it into account.

One may observe the complexity of erythropoiesis through the model we propose. Erythroid progenitors and erythrocytes contribute to the control of growth factor concentrations in blood, which in turn regulate intracellular mechanisms of cell fate (self-renewal, differentiation, apoptosis). We complete the model of erythropoiesis by specifying how intracellular regulatory mechanisms influence erythroid progenitor fate.

As described in Section 2, self-renewal, differentiation and apoptosis rates depend on levels of activated Erk and Fas, denoted by E_i and F_i , the subscript i referring to a given sub-population. Moreover, apoptosis rate is also inhibited by Epo independently of the intracellular network based on Erk and Fas. Hence, functions s_i , d_i and a_i are defined as

$$s_i = s(E_i, F_i), \quad d_i = d(E_i, F_i), \quad a_i = a(E_i, F_i) f_{aEpo}(Epo), \quad (12)$$

where functions s , d and a define self-renewal, differentiation, and apoptosis rates, respectively, for given Erk and Fas levels. The function f_{aEpo} describes a direct mechanism of apoptosis inhibition by Epo, which is independent of the intracellular regulatory network. It is assumed to be bounded, positive and decreasing.

Dynamics of erythroid progenitors, described by Equations (4)–(5), are then coupled to protein levels (11) through erythrocyte dynamics in (6), growth factor concentration evolution in (7)–(8), and self-renewal, differentiation and apoptosis rates definitions in (9) and (12). This set of equations forms the multi-scale model of erythropoiesis we study below.

4.2. Existence of Steady States

We investigate the existence of steady states for the system formed with (4)–(9), (11) and (12). It should be noted that existence of such solutions is not straightforward. Indeed, denote by P_i^* the steady state values of (4)–(5), M^* the steady state value of (6), Epo^* and GC^* the steady state values of (7)–(8), and E_i^* and F_i^* the steady state values of (11). We also introduce the notations

$$s_i^* = s(E_i^*, F_i^*), \quad d_i^* = d(E_i^*, F_i^*), \quad a_i^* = a(E_i^*, F_i^*) f_{aEpo}(Epo^*).$$

Then, P_i^* , $i = 1, \dots, n$, exist if and only if

$$\begin{cases} (d_1^* + a_1^* - s_1^*) P_1^* = HSC, \\ (d_i^* + a_i^* - s_i^*) P_i^* = 2d_{i-1}^* P_{i-1}^*, \quad i = 2, \dots, n. \end{cases}$$

Hence, using (9), P_i^* exists for $i = 1, \dots, n$ provided that

$$s_i^* < \frac{1}{2},$$

and P_i^* is given by

$$P_1^* = \frac{HSC}{1 - 2s_1^*}, \quad P_i^* = \frac{2d_{i-1}^*}{1 - 2s_i^*} P_{i-1}^*, \quad i = 2, \dots, n.$$

Then, M^* , Epo^* and GC^* are uniquely defined by

$$M^* = \frac{d_n^*}{\delta} P_n^*, \quad Epo^* = \frac{f_{Epo}(M^*)}{k_{Epo}}, \quad GC^* = \frac{f_{GC}(M^*)}{k_{GC}}.$$

Yet, implicitly, all the above steady state values, and in particular P_n^* , Epo^* and GC^* , are functions of E_i^* and F_i^* , for $i = 1, \dots, n$, through the steady state

values of the different rates s_i^* , d_i^* and a_i^* . Since E_i^* and F_i^* are solutions of system

$$\begin{cases} (\alpha(Epo^*, GC^*) + \beta(E_i^*)^k)(1 - E_i^*) - aE_i^* - bE_i^*F_i^* & = 0, \\ \gamma_i(P_n^*)(1 - F_i^*) - cE_i^*F_i^* - dF_i^* & = 0, \end{cases}$$

which has been shown to have 1 to 3 solutions when α and γ are constant (see Section 2), it follows that determining steady states for the full model is equivalent to solving a system in the form

$$\begin{cases} E_i^* & = \varphi_i(E_1^*, \dots, E_n^*, F_1^*, \dots, F_n^*), \\ F_i^* & = \psi_i(E_1^*, \dots, E_n^*, F_1^*, \dots, F_n^*), \end{cases}$$

for all $i = 1, \dots, n$. Functions φ_i and ψ_i are some unknown functions. In a general case such a system cannot be solved.

For the sake of simplicity, suppose α is given by

$$\alpha(Epo, GC) = \alpha_0 + f(Epo) + g(GC),$$

where $\alpha_0 > 0$ accounts for Erk activation when erythropoietin and glucocorticoids are low. Since erythropoietin and glucocorticoids are not the only activators of Erk, this assumption is biologically relevant. Functions f and g are bounded nonnegative increasing functions, for instance, Hill functions, with $f(0) = g(0) = 0$. Similarly, suppose γ_i is given by

$$\gamma_i(P_n) = \gamma_0 + \mu_i \bar{\gamma}(P_n),$$

where γ_0 is a constant source of Fas activation independent of mature progenitor cell production of Fas ligand, and μ_i is a parameter accounting for sensitivity of Fas activation to cell maturity. The function $\bar{\gamma}$ is assumed to be nonnegative, bounded and increasing, with $\bar{\gamma}(0) = 0$ and $\gamma(P_n) \leq 1$.

With these assumptions, we can apply the Implicit Function Theorem to find steady states of the full model. Suppose that in the steady state, values of Epo^* and GC^* are such that $f(Epo^*) + g(GC^*)$ is very small, close to zero. Moreover, μ_i are supposed to be small parameters.

We first note that the following system,

$$\begin{cases} (\alpha_0 + \beta(E_i^*)^k)(1 - E_i^*) - aE_i^* - bE_i^*F_i^* & = 0, \\ \gamma_0(1 - F_i^*) - cE_i^*F_i^* - dF_i^* & = 0, \end{cases} \quad (13)$$

has one to three solutions, depending on the values of α_0 and γ_0 . This has been obtained in Section 2, for $\alpha = \alpha_0$ and $\gamma = \gamma_0$, see System (2). Denote by $(E^{*,0}, F^{*,0})$ one of these potential solutions. Then for every pair $(E^{*,0}, F^{*,0})$, there exists a unique value of s_i^* , d_i^* and a_i^* , and consequently of P_i^* , $i = 1, \dots, n$, M^* , Epo^* and GC^* .

As μ_i increases away from zero, the Implicit Function Theorem gives the existence of steady states for the full model. These steady states are small perturbations of the above mentioned steady states, based on $(E^{*,0}, F^{*,0})$. Hence,

stability does not change, and steady states of the full system are stable (respectively, unstable) if steady states of (4)–(9), (12) and (13) are stable (respectively, unstable). And (13) has up to 2 stable steady states for all $i = 1, \dots, n$.

We can then state that full system formed with (4)–(9), (11) and (12) has up to 2^n stable steady states. This number may appear large, yet it does not take into account biological constraints. An interested reader can find a detailed analysis of a similar system in [14].

During the process of maturation, erythroid progenitors lose their ability to self-renew [12], thus immature cells are more inclined to self-renewal and mature ones are more inclined to differentiation. Hence, among all possible stable steady states only those, characterised by a certain integer j , $1 \leq j \leq n$, such that cells in the first j sub-populations (corresponding to variables P_1 to P_j) preferentially self-renew (let us call them self-renewing sub-populations), and cells in the last $n - j$ sub-populations (corresponding to variables P_{j+1} to P_n) preferentially differentiate (let us call them differentiating sub-populations), are biologically reasonable. It reduces the number of biologically meaningful stable steady states to n . Moreover, it seems natural to expect that in normal erythropoiesis the number of mature cells is larger than the number of immature cells, so we impose the conditions $P_i^* < P_{i+1}^*$, which are equivalent to

$$\frac{2d_i^*}{1 - 2s_{i+1}^*} > 1, \quad i = 1, \dots, n - 1.$$

Thus the multi-scale model formed with (4)–(9), (11) and (12) has, generally speaking, several (from 1 up to n) stable steady states, which satisfy the biological constraints discussed above.

The next two sections are devoted to parameter values estimations and to numerical simulations of the system obtained above. We focus our attention, in particular, on anaemia situations.

5. Parameter Values

A typical situation of stress erythropoiesis is anaemia: a lack of red blood cells, or haemoglobin. It can be either induced, for instance by killing erythrocytes, which can be obtained for instance with phenylhydrazine, or by bleeding, or disease-related. A lot of haematological diseases are characterised by or associated with severe anaemia, such as aplastic anaemia or some leukaemias.

The nature of the induced anaemia can be very different, according to the method used to urge it. Finch et al. [15] noticed that the way haematocrit evolves following the anaemia induction, and in particular the speed of the return to the equilibrium, strongly depends on its strength. In other words, the more red blood cells are removed from the body, the stronger response to anaemia is. Results of experiments on mice with phenylhydrazine-induced anaemia obtained in Cherukuri et al. [9] are presented in Figure 4. One can observe that, following the anaemia, the erythrocyte count quickly increases and, although still not at its equilibrium, decreases once again on day 11 before

finally reaching normal values from day 18 up to the end of experiments. This surprising decrease (days 11 to 18) will be investigated in Section 6: we will look for feedback controls responsible for it.

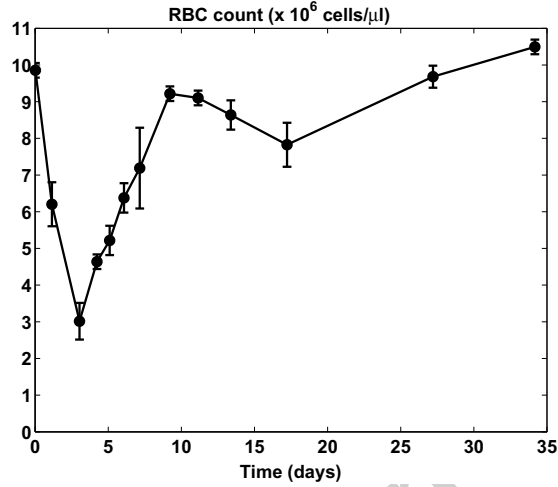


Figure 4: Phenylhydrazine-induced anaemia in mice, adapted from Cherukuri et al. [9]. Two injections (60mg/kg) are administered intraperitoneally at days 0 and 1. Mean values among six mice are presented with error bars. Initial value of red blood cell count (before starting the experiment) is about 10^7 cells. μ l $^{-1}$.

We consider the model of erythropoiesis that consists of Equations (4)-(6) describing immature and mature blood cell dynamics, Equations (7)-(8) describing growth factors dynamics, and Equation (11) accounting for intracellular regulatory mechanisms.

We determine functions and parameter values of the model. Some parameters are rather easily accessible, whereas other parameters and most feedback functions are usually unavailable. We distinguish between these two kinds of values.

5.1. Estimations based on existing data

Among easily accessible parameter values, the mortality rate of erythrocytes (δ in equation (9)) is the first for which a value can be assigned. Since erythrocyte average lifespan in mice equals 40 days, we chose $\delta = 1/40$ d $^{-1}$.

Let now focus on growth factor dynamics system (7)-(8). In mice the half-life of erythropoietin is about 180 minutes [31]. The half-life of glucocorticoids ranges in a wide interval, yet 90 minutes can be considered as reasonable for short-term glucocorticoids [22] (that is glucocorticoids acting for a short time), like cortisol, which are likely to be involved in stress erythropoiesis [6]. Using the definition of half-life, we compute degradation constants: consider a substance

that degrades with constant rate ν , then its dynamics can be described by the equation,

$$\frac{dx}{dt} = -\nu x,$$

whose solution is $x(t) = x_0 e^{-\nu t}$. The half-life is the time $T_{1/2}$ such that

$$x(T_{1/2}) = \frac{x_0}{2},$$

which gives $\nu = \ln(2)/T_{1/2}$. Using the above estimations for the half-life of erythropoietin and glucocorticoids, we obtain the following values for the degradation constants,

$$k_{Epo} = 5.55 \text{ d}^{-1}, \quad k_{GC} = 11.1 \text{ d}^{-1}.$$

The functions f_{Epo} and f_{GC} in (7) and (8), accounting for growth factor production terms, are supposed to be Hill functions [7, 27],

$$f_{Epo}(M) = f_{Epo}^0 \frac{\theta_{Epo}^{q_E}}{\theta_{Epo}^{q_E} + M^{q_E}}, \quad f_{GC}(M) = f_{GC}^0 \frac{\theta_{GC}^{q_G}}{\theta_{GC}^{q_G} + M^{q_G}}.$$

During anaemia Epo blood concentrations increase by 2-3 orders [32]. To our knowledge, variations of glucocorticoids are less important, but exact values are not available. We then chose parameters of functions $f_{Epo}(M)$ and $f_{GC}(M)$ that allowed us to obtain such variations of Epo and GCs in anaemia simulations we carried out. All these parameters are listed in Table 1.

Table 1: Values of the parameters used to numerically compute erythrocyte count and growth factor levels. N.U means “no unit is relevant”.

Parameter		Value	Unit
δ	mortality rate of erythrocytes	0.025	d^{-1}
k_{Epo}	degradation rate of Epo	5.55	d^{-1}
k_{GC}	degradation rate of GC	11.1	d^{-1}
f_{Epo}^0	maximum value of f_{Epo}	7130	$\text{mU} \cdot \mu\text{l}^{-1}$
θ_{Epo}	threshold value of f_{Epo}	4.63×10^6	$\text{cells} \cdot \mu\text{l}^{-1}$
q_E	sensitivity of f_{Epo}	7	N.U.
f_{GC}^0	maximum value of f_{GC}	2930	$\text{mU} \cdot \mu\text{l}^{-1}$
θ_{GC}	threshold value of f_{GC}	7.69×10^6	$\text{cells} \cdot \mu\text{l}^{-1}$
q_G	sensitivity of f_{GC}	6	N.U.

As obtained in Section 4.2, the model we consider has from 1 up to n stable steady states. Not all steady states are biologically meaningful and one of these numerous steady states can be selected by taking into consideration a realistic proportion between the daily influx of haematopoietic stem cells (input of the model) and erythrocyte count in mice (output of the model). From Crauste et al. [11], the ratio M^*/HSC between normal erythrocyte count and

HSC daily influx can be estimated in the order of 10^5 . The number of self-renewing sub-populations (see discussion at the end of Section 4.2) allows to select the appropriate steady state. We carried out several simulations with different numbers of self-renewal-inclined sub-populations and we obtained a correct ratio M^*/HSC for $n = 8$ and the case of 4 immature preferentially self-renewing sub-populations, and consequently 4 mature differentiation-inclined sub-populations.

5.2. Intracellular regulatory network

Let first focus on the part of the intracellular regulatory system (11) independent of feedback functions. Variables E and F are dimensionless and the parameter values we use are deduced from numerical simulations since no data are available in the literature. They are

$$\begin{aligned} k &= 2, & \beta &= 40 \text{ d}^{-1}, & a &= 2 \text{ d}^{-1}, \\ b &= 40 \text{ d}^{-1}, & c &= 10 \text{ d}^{-1}, & d &= 2.5 \text{ d}^{-1}. \end{aligned} \quad (14)$$

With these values, the intracellular regulatory network may have three steady states for given α and γ (Figure 2), two steady states being stable.

As mentioned in previous sections, System (11), describing intracellular regulatory network, in which α stands for Erk activation by Epo and GCs, and γ stands for Fas activation by FasL, can have either one or two stable steady states. Thus, primordially bistable system can temporarily lose its bistability when values of parameters α and γ change, like in stress situations. For the parameters of the intracellular regulatory network mentioned in (14), we found numerically the set of (α, γ) values, for which System (11) has a bistable behaviour (domain D_1 in Figure 5).

After determining system parameters (see below), we numerically tested two cases: first when intracellular regulatory network always keeps a bistable behaviour during anaemia, independently of the values of α and γ , and second when for some extreme values of α and γ the bistability is temporarily lost and the intracellular regulatory network has only one stable steady state. The first case corresponds to variations of α and γ in the rectangular domain D_2 in Figure 5 that is entirely inside the bistability area. The second case corresponds, for instance (this is what was tested), to variations of α and γ in the domain D_3 that partially exits D_1 . If a system trajectory goes through these out-of- D_1 parts of D_3 , then the bistability of System (11) is lost for the corresponding values of (α, γ) . We investigated the consequences of these two distinct situations on the response to anaemia.

In the second case the response of the system was stronger but qualitatively the same as the one obtained in the first case. We tried to increase out-of- D_1 parts of domain D_3 through which the trajectory goes and we obtained that beyond certain thresholds (i.e. if the trajectory stays long enough outside the domain D_1), the solution could not come back to its initial state, the solution changed an attractor and went definitely to another steady state, or in other words, the system switched to single stable steady state regimen. The system

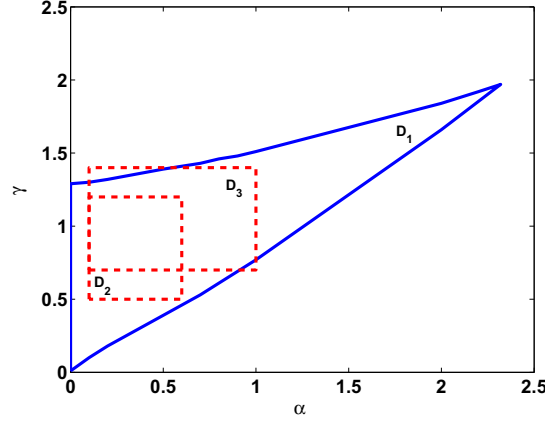


Figure 5: Intracellular system (11) has a bistable behaviour for (α, γ) inside D_1 . Two examples of (α, γ) variations are tested numerically, domains D_2 and D_3 , when bistability can be temporarily lost.

would then lose its biological meaning (the balance between self-renewal and differentiation would be broken) and consequently we decided to focus only on the first case (α and γ range in D_2) and we present numerical simulations only for this case.

Let now concentrate ourselves on the choice of functions α and γ .

For the sake of simplicity, we supposed that FasL exerts the same feedback control on Fas activation for all progenitor sub-populations, which implies that $\gamma_i(P_n)$ in (11) is independent of i : $\gamma_i(P_n) = \gamma(P_n)$ for all $i = 1, \dots, n$.

The system trajectory represented on (α, γ) -plane stays inside domain D_2 during erythrocyte recovery. The domain D_2 is characterised by $\alpha \in [0.1, 0.6]$, $\gamma \in [0.5, 1.2]$, see Figure 5. Recall that $\alpha = \alpha(Epo, GC)$ and $\gamma = \gamma(P_n)$. We suppose $\alpha(Epo, GC) = \alpha_0 + f(Epo) + g(GC)$, where α_0 is constant and $f(Epo)$, $g(GC)$ are Hill functions,

$$f(Epo) = f_{max} \frac{Epo^{q_f}}{\theta_f^{q_f} + Epo^{q_f}}, \quad g(GC) = g_{max} \frac{GC^{q_g}}{\theta_g^{q_g} + GC^{q_g}}. \quad (15)$$

Function $\gamma(P_n)$ is supposed to be a Hill function, given by

$$\gamma(P_n) = \gamma_{min} + (\gamma_{max} - \gamma_{min}) \frac{P_n^{q_\gamma}}{\theta_\gamma^{q_\gamma} + P_n^{q_\gamma}}. \quad (16)$$

No information could allow us to determine the shape of such functions. The choice of Hill functions lies on the interest of these functions in describing kinase cascades and, more generally, biological phenomena with saturation effects. Parameter values of functions $\alpha(Epo, GC)$ and $\gamma(P_n)$ are given in Table 2. They were deduced from numerical simulations.

Table 2: Parameters of the intracellular regulatory network, functions $\alpha(Epo, GC) = \alpha_0 + f(Epo) + g(GC)$ and $\gamma(P_n)$, defined in (15) and (16). N.U means “no unit is relevant”.

Parameter		Value	Unit
k	sensitivity of Erk self-activation	2	N.U.
β	rate of Erk self-activation	40	d ⁻¹
a	Erk degradation rate	2	d ⁻¹
b	suppression of Erk expression rate	40	d ⁻¹
c	suppression of Fas expression rate	10	d ⁻¹
d	Fas degradation rate	2.5	d ⁻¹
α_0	constant Erk activation rate	0.1	d ⁻¹
f_{max}	maximum value of $f(Epo)$	0.25	d ⁻¹
q_f	sensitivity of $f(Epo)$	6	N.U.
θ_f	threshold value of $f(Epo)$	100	mU. μ l ⁻¹
g_{max}	maximum value of $g(GC)$	0.25	d ⁻¹
q_g	sensitivity of $g(GC)$	2	N.U.
θ_g	threshold value of $g(GC)$	49.4	mU. μ l ⁻¹
γ_{min}	minimum value of $\gamma(P_n)$	0.5	d ⁻¹
γ_{max}	maximum value of $\gamma(P_n)$	1.2	d ⁻¹
q_γ	sensitivity of $\gamma(P_n)$	3	N.U.
θ_γ	threshold value of $\gamma(P_n)$	1.14×10^6	cells. μ l ⁻¹

5.3. Self-renewal, differentiation and apoptosis rates

From Equations (9), (10) and (12), self-renewal, differentiation and apoptosis rates are given, for $i = 1, \dots, n$, by

$$\begin{cases} s_i &= (1 - a_i) p_s(E_i, F_i), \\ d_i &= 1 - s_i - a_i, \\ a_i &= a(E_i, F_i) f_{aEpo}(Epo). \end{cases} \quad (17)$$

The dependence upon Erk and Fas is defined through function $p_s(E, F)$, which describes how the probability of self-renewal depends upon Erk and Fas, and function $a(E, F)$, which describes how apoptosis rate depends on Erk and Fas. The direct action of Epo on apoptosis rate is determined by $f_{aEpo}(Epo)$. Hence, the three functions p_s , a and f_{aEpo} entirely determine the three rates.

The function f_{aEpo} is supposed to be decreasing and bounded. In order to describe the effect of large Epo variations (quick changes from 5 to 1000 mU. μ l⁻¹), we chose a Hill function of the logarithm of Epo, given by,

$$f_{aEpo}(Epo) = 0.2 + \frac{0.73 \times 1.1^{9.2}}{1.1^{9.2} + (\log_{10}(Epo))^{9.2}}, \quad (18)$$

the parameters being dimensionless, except the threshold value 1.1, which is expressed in mU. μ l⁻¹. Parameters have been chosen so that $f_{aEpo}(Epo)$ in the steady state Epo^* equals 0.9 and numerical simulations fit correctly experimental data from Figure 4.

For the sake of simplicity, we supposed functions $p_s(E, F)$ and $a(E, F)$ to be functions of one variable, $p_s(E, F) = p_s(E - F)$ and $a(E, F) = a(F - E)$. The function p_s is supposed to take larger values when Erk levels are high, whereas the value of a is more important when Fas levels are high. Consequently, both functions are supposed to be increasing. Moreover, they are positive and we assumed the following form,

$$z(x) = z_{min} + \frac{(z_{max} - z_{min})(x + 1)^{n_z}}{\theta_z^{n_z} + (x + 1)^{n_z}}, \quad x \in [-1, 1].$$

Before giving values of the parameters z_{min} , z_{max} , n_z and θ_z associated with functions p_s and a , let us illustrate how the roles of Erk and Fas are investigated through these functions.

Let us recall that we assumed functions γ_i do not depend on the index i . Hence, from (11) it follows that all sub-populations have the same steady state values (E^*, F^*) , which do not depend on i . Moreover, by assuming that α and γ evolve in the restricted domain D_2 , we ensure the existence of two stable steady states for System (11), one in which Erk levels are higher than Fas levels, and the other one with higher Fas levels. These two steady states (E^*, F^*) provide two distinct values of the variable $F^* - E^*$, one positive and one negative. The positive value is associated with cell differentiation, whereas the negative one corresponds to cell self-renewal. Hence, the positive value of $F^* - E^*$ characterises differentiation-inclined erythroid progenitors, that is mature cells, and the negative one self-renewal-inclined erythroid progenitors, that is immature cells.

During anaemia, concentrations of Erk and Fas vary, therefore values of $F - E$ vary as well. Carrying out simulations however, we observed that variations of $F - E$ were limited to neighborhoods of the two stationary points $F^* - E^*$, and did not range in the whole interval $[-1, 1]$. This means that variations of functions $p_s(E - F)$ and $a(F - E)$ are only relevant on these neighborhoods of $F^* - E^*$. Consequently, in order to determine the roles of Erk and Fas on the response to anaemia, we considered three cases describing three different ways of acting on self-renewal, differentiation and apoptosis rates, based on variations of p_s and a in the neighborhoods of the steady state values.

In the first case $p_s(E - F)$ and $a(F - E)$ vary slightly on both neighborhoods of the steady states. In the second case $p_s(E - F)$ (respectively $a(F - E)$) varies a lot near the steady state corresponding to Erk prevalence, i.e. $F^* - E^* < 0$ (respectively, Fas prevalence, i.e. $F^* - E^* > 0$), and is almost constant near the other steady state. Biologically it can be interpreted as follows: in critical situations Erk and Fas importantly modify the progenitor self-renewal rate of immature but not of mature cells, and apoptosis rate is strongly modified in mature cells but not in immature ones. The third case is opposite to the second one. It should be noted that the assumption on the three rates that confines them in the interval $[0, 1]$, limits maximum values of functions p_s and a , so the fourth possible case, when the functions vary a lot on both neighborhoods is ineligible. Simulations indicated that the response obtained in the first case is weak, that is the system takes more time to come back to the equilibrium.

Second case seemed to us biologically more realistic than the third one, hence we chose to use only the second case for the numerical simulations. Nevertheless, it can be noted that the simulation of the third case showed a weaker response, i.e. slower erythrocyte count dynamics, though the rates displayed different dynamics.

In order to obtain a good fit of experimental data, functions $p_s(E - F)$ and $a(F - E)$ used for the simulations are

$$p_s(x) = 0.1 + \frac{1.2 \times x^{40}}{1.7^{40} + x^{40}}, \quad a(x) = 0.12 + \frac{1.02 \times x^{40}}{1.5^{40} + x^{40}}.$$

Units of 0.12 and 1.02 for function a are d^{-1} , other parameters are dimensionless values.

5.4. Steady state values

Since we are going to confront the simulation results with experimental data presented in Figure 4, we tried to get equilibrium value of erythrocyte count $M^* = 10^7 \text{ cells} \cdot \mu\text{l}^{-1}$. This implied $HSC = 80 \text{ cells} \cdot \mu\text{l}^{-1} \cdot \text{d}^{-1}$. As initial condition for the number of erythrocytes we took 30% of its equilibrium value, which corresponds to the anaemia presented in Figure 4 (see value of RBC count on day 3). Equilibrium values are taken as initial conditions for all other system variables. Steady state values of the main system components, obtained through the simulation, are presented in Table 3.

Table 3: Steady state values of the main variables of the system.

Steady states		Value	Units
Erythrocyte count	M^*	10^7	$\text{cells} \cdot \mu\text{l}^{-1}$
Reticulocyte count	P_8^*	4.75×10^5	$\text{cells} \cdot \mu\text{l}^{-1}$
Erythropoietin level	Epo^*	5.7	$\text{mU} \cdot \mu\text{l}^{-1}$
Glucocorticoids level	GC^*	44.6	$\text{mU} \cdot \mu\text{l}^{-1}$
Fas – Erk level for immature cells	$F^* - E^*$	-0.66	N.U.
Fas – Erk level for mature cells	$F^* - E^*$	0.48	N.U.
Activation rate of Erk $\alpha(Epo^*, GC^*)$	α^*	0.21	d^{-1}
Activation rate of Fas $\gamma(P_n^*)$	γ^*	0.55	d^{-1}
Self-renewal rate of immature cells	s^*	0.44	d^{-1}
Self-renewal rate of mature cells	s^*	0.06	d^{-1}
Differentiation rate of immature cells	d^*	0.45	d^{-1}
Differentiation rate of mature cells	d^*	0.53	d^{-1}
Apoptosis rate of immature cells	a^*	0.11	d^{-1}
Apoptosis rate of mature cells	a^*	0.41	d^{-1}

As shown in Table 3, in normal erythropoiesis reticulocyte count is 20-fold smaller than erythrocyte count. Progenitor sub-populations P_1, \dots, P_7 are much smaller than P_8 (not shown here). The model predicts that 44% of immature progenitors self-renew per day (only 6% of mature progenitors per day), which

allows the conclusion that mature progenitors mainly lost their ability to self-renew. Apoptosis rate is high in mature cells ($41\% \text{ d}^{-1}$), whereas it is only $11\% \text{ d}^{-1}$ in immature cells. About 53% of mature and 45% of immature progenitors differentiate per day, providing that the differentiation remains important in all erythroid cells. Thus, in normal erythropoiesis, immature progenitor subpopulations are characterised by weak apoptosis and comparable self-renewal and differentiation rates. Mature progenitors, however, preferentially differentiate with high apoptosis.

The next section is devoted to numerical simulations of phenylhydrazine-induced anaemia.

6. Simulation of Phenylhydrazine-Induced Anaemia and Comparison with Experimental Data

Using parameter values obtained in the previous section, we numerically computed solutions of system formed with Equations (4) to (8) and Equation (11), for an anaemia-induced situation: it is assumed that at the beginning of the numerical computations (day 0) the erythrocyte count is lower than its equilibrium value (30% of its equilibrium) due to previous phenylhydrazine injections. Simulations were carried out using MATLAB and results are presented in Figures 6 to 10.

First, dynamics of main variables of the system and of some relevant rates are illustrated: erythrocyte and reticulocyte counts in Figure 6, erythropoietin and glucocorticoid levels in Figure 7, Erk and Fas levels in Figure 8, self-renewal, differentiation and apoptosis rates in Figure 9. Explanations on the dynamics of the system are proposed. Then results are confronted to experimental data from Figure 4 in Figure 10.

All simulations start at day zero. For the sake of clarity, equilibrium values are shown on days -1 to 0.

6.1. Erythrocyte and reticulocyte counts

Erythrocyte count (solid line) and reticulocyte count (dash line) dynamics are presented in Figure 6.

Following the anaemia, erythrocyte count quickly increases and reaches a maximum value (lower than the equilibrium value) after 7 days, then stays there up to day 10. Afterwards, erythrocyte count slowly decreases (days 10 to 17). Quick increase is observed between days 17 to 21, followed by a gradual return to the equilibrium. Although erythrocyte count globally increases between day 0 and day 30, it should be noted that 30 days after anaemia the erythrocyte count is still below its equilibrium value.

At day 0, the reticulocyte count increases to reach a maximum value that equals approximately four-fold of its equilibrium value on day 4, then comes back to its steady state and keeps on decreasing. On day 17, when erythrocyte count is decreasing, the number of reticulocyte increases once again, though less importantly this time.

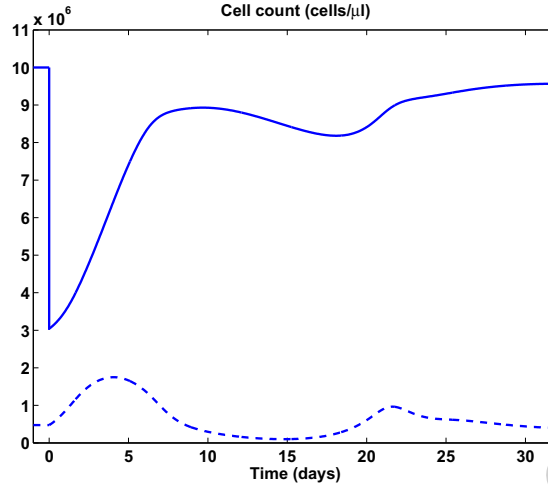


Figure 6: Anaemia simulation. Erythrocyte and reticulocyte count dynamics. Solid curve represents erythrocyte count, dash curve represents reticulocytes. Equilibrium value of erythrocyte count used in the simulation is $M^* = 10^7 \text{ cells} \cdot \mu\text{l}^{-1}$.

The first increase of reticulocyte count (up to day 4) is due to a strong increase of mature progenitor differentiation, see Figure 9.B. Explanations on the behavior of erythrocyte and reticulocyte counts on day 17 are however less straightforward and will be given later in Section 6.5, when confronting the results with experimental data.

6.2. Growth factors dynamics

In Figure 7, erythropoietin and glucocorticoid dynamics are shown. Growth factor levels are strongly perturbed (large increase) during the first five days following the anaemia, this perturbation being characterised by a sharp increase of both concentrations on day 1, when the organism lacks erythrocytes. Then values of Epo and GCs levels smoothly return to their equilibria, with small perturbations, in particular they both increase once again on day 17, due to the fall in erythrocyte count (Figure 6).

As it will be noted in the following sections, two different actions of Epo and GCs appear in the response to anaemia. First, in the early stages of the response to anaemia (between days 0 and 5) mainly Epo inhibits apoptosis (Figure 9), leading to high proliferation of immature progenitors. Second, from day 6 up to the end of the response, Epo and GCs levels are closer to their equilibrium values and they regulate erythropoiesis mainly through Erk-Fas regulation (Figure 8).

6.3. Erk and Fas levels

Dynamics of variable $F - E$ and feedback controls expressed by α and γ are presented in Figure 8. Values of $F - E$ in all mature (respectively, in all

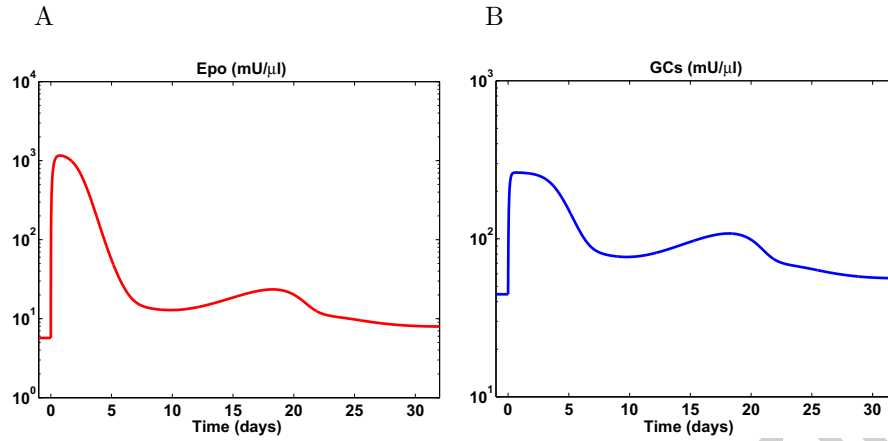


Figure 7: Anaemia simulation. Dynamics of growth factors, shown on logarithmic scale.

immature) sub-populations are similar because the feedback by FasL has been supposed to be the same on all cells (see Section 5.2).

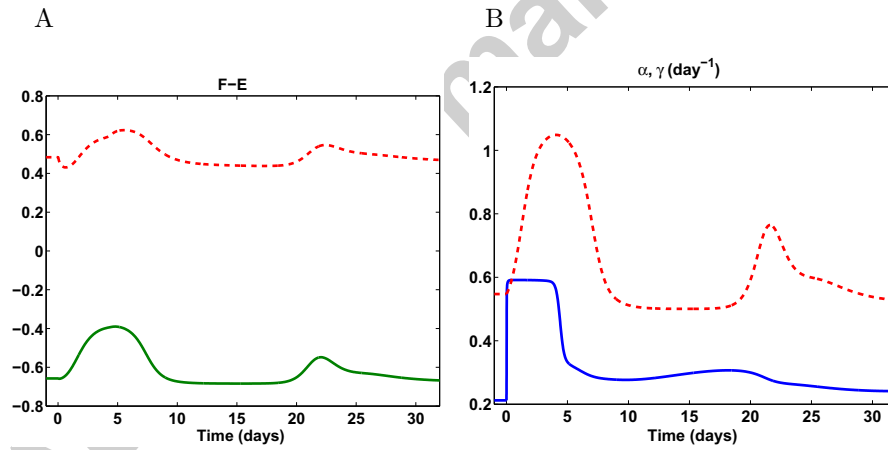


Figure 8: Anaemia simulation. Panel A: Dynamics of $F - E$ for self-renewing (green solid curve) and differentiating (red dash curve) sub-populations. Panel B: Dynamics of $\alpha(Epo, GC)$ (blue solid curve) and $\gamma(P_n)$ (red dash curve).

On the first day following anaemia the quantity $F - E$ decreases. This is more clearly observed for mature cells (red dash curve), yet it also occurs for immature cells (green solid curve). This is due to high values of α (Panel B), the feedback function controlling Erk production. Then, $F - E$ increases and reaches its extreme values after 5-6 days following anaemia induction. As one can observe on Panel A, between days 9 and 19 the difference $F - E$ has values

below its equilibria, which is due to the regulation through α and γ .

Production of Erk, the feedback control expressed by α , is at its maximum during the first four days, while γ (production of Fas) is increasing. Then, α sharply decreases almost down to its equilibrium, while γ decreases smoothly and reaches its minimum value, where it stays from day 10 up to day 18. On day 18, a new increase of γ is observed, due to the increase of the reticulocyte count (Figure 6). Two different behaviors are observed in α and γ dynamics: fast changes (α on days 1 and 4) and modest variations (γ between days 1 and 8, and days 18 and 25). Fast changes of α are directly due to sharp Epo and GCs dynamics (see Figure 7), while modest γ dynamics is due to modest evolution of reticulocyte count (see Figure 6).

6.4. Self-renewal, differentiation and apoptosis rates

Self-renewal, differentiation and apoptosis rates are presented in Figure 9. The three rates exhibit important fluctuations. Their dynamics for immature and mature cell populations are different.

Self-renewal rate varies a lot for all cells. At first sight, it seems not to be the case for mature cells, yet self-renewal equilibrium value is small and the variations represent a two-fold increase of the equilibrium value. Such important variations are also observed for the two other rates. Moreover, two different types of changes in values of the rates appear in Figure 9. First, sharp variations appear between days 0 and 1: they are strong, for instance, for mature sub-populations (red dash curves in Figure 9). Then, after day 1, variations are more gradual, sometimes with large amplitudes.

Taking into account the nature of the feedback controls, we conclude that sudden sharp variations in the three rates right after the induction of anaemia are due to direct inhibition of apoptosis by Epo, independently of the intracellular network based on Erk and Fas, and gradual variations that occur later (after day 2) are due to Erk and Fas regulation. During the first six days these gradual variations are observed for the self-renewal rate (Panel A) and the differentiation rate (Panel B) of immature cells. During days 6-32, the three rates keep on varying gradually, which is due to Erk and Fas variations. These fluctuations are important, suggesting a strong dependence of the rates on Erk and Fas (which at the same time vary modestly), and last longtime (40-45 days, not shown here). These conclusions must however be completed by the fact that the influence of Epo on apoptosis rate is observed as long as its levels are not back to equilibrium value, especially for immature self-renewing sub-populations (Figure 9.C).

It should be noted as well that differentiation in our model is a choice by default, i.e. a cell that is protected against apoptosis and which does not self-renew differentiates.

6.5. Confrontation to experimental data

Simulation results and experimental data are presented in Figure 10. The blue dash curve represents the simulation discussed above (Figure 6), the black

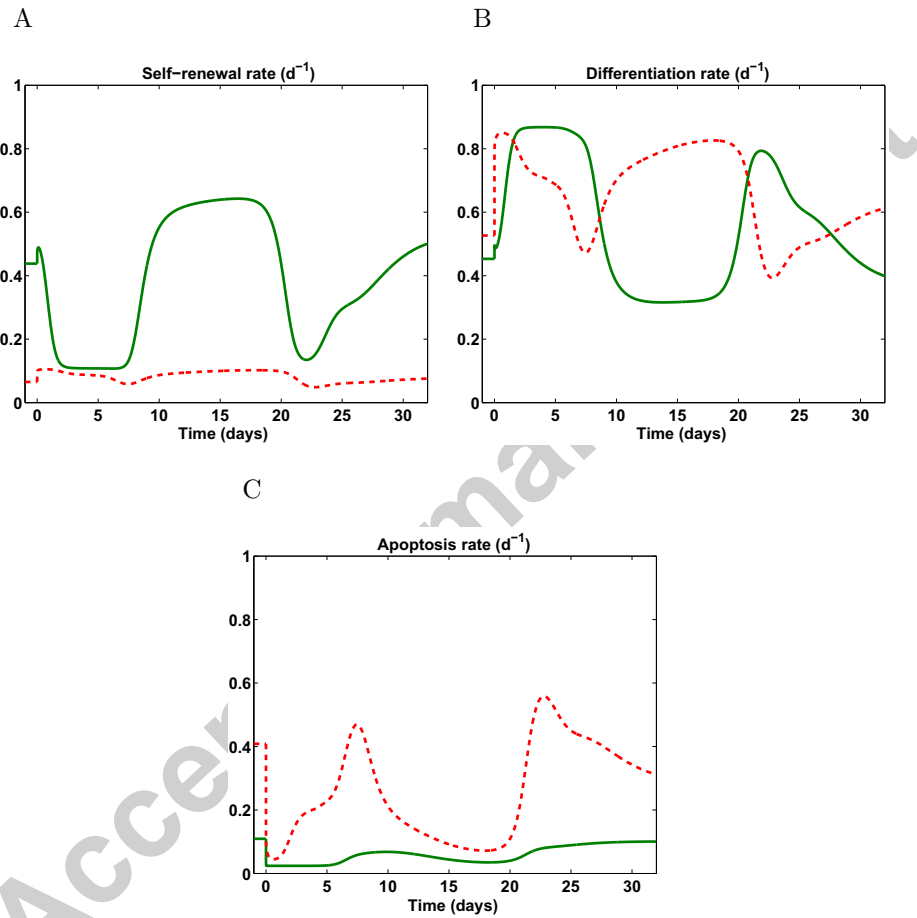


Figure 9: Anaemia simulation. Self-renewal, differentiation and apoptosis rates of immature self-renewing (green solid curve) and mature differentiating (red dash curve) sub-populations.

solid line represents the outcome of experiments by Cherukuri et al. [9] (Figure 4).

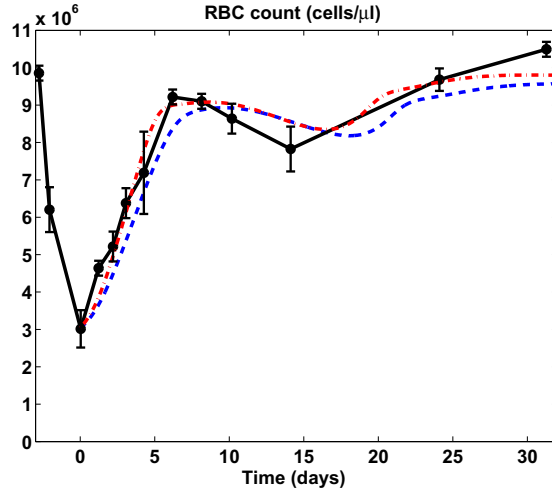


Figure 10: Anaemia simulations. Erythrocyte count dynamics obtained by Cherukuri et al. [9] in experiments on induced anaemia in mice (black circled solid line), obtained in simulations carried out with $\delta = 1/40 \text{ d}^{-1}$ (blue dash curve) and with $\delta = 1/30 \text{ d}^{-1}$ (red dash-dot curve).

Let focus on the simulated blue dash curve. First, from day 0 to day 7, the computed erythrocyte count increases as fast as observed in the experiments, with only one day delay. From day 10, simulated erythrocyte count decreases in spite of its low value (lower than equilibrium). Similar phenomenon is observed in the experiments (black solid line) from day 8 to 15. The cause of such a decrease in cell numbers although the erythrocyte count is still lower than normal is investigated in the following.

In Figure 6, reticulocyte count starts decreasing at day 4. Figure 9 shows that during first four days apoptosis rate is below its equilibrium for mature cells, whereas both self-renewal and differentiation rates are above their equilibrium values. This results in an increase of the number of mature progenitors (not shown here). However, for immature cells the picture is a bit different, self-renewal rate increases a little bit on the first day and then decreases a lot due to high $F - E$ values (Figure 8.A), differentiation rate is higher than at equilibrium, apoptosis rate is lower than at equilibrium. This results in a decrease of the number of immature progenitors (not shown here). Hence, on day 4 the system starts lacking immature cells to maintain the increase of mature progenitors that triggers a decrease of the latter and, thus, of reticulocytes. Apoptosis of mature progenitors is high during days 6-8 (Figure 9.C), whereas differentiation rate is low (Panel B) and self-renewal is about its steady state (Panel A). This makes reticulocyte count decrease even faster (Figure 6), go below its equilibrium on day 8, where it stays up to day 19. This, in turn, decreases the supply of

mature erythrocytes that results in the reduction of erythrocyte count observed between day 10 and day 18. Thus, our model suggests that this decrease of erythrocyte count is a consequence of low self-renewal rate of immature cells during first seven days and of the high apoptosis of mature cells during days 6-8. This, in turn, is due to a high value of $F - E$ (Figure 8.A) and not to Epo control of apoptosis, which is below its equilibrium during these days and should, in contrary, decrease apoptosis rate (Figure 11). Consequently, this decrease (days 10-18) of the erythrocyte count can be explained by Erk-Fas regulation. It can be compared to the quick increase of erythrocyte count following the anaemia, which is clearly due to an inhibition of progenitor apoptosis by Epo, independently of Erk-Fas regulation.

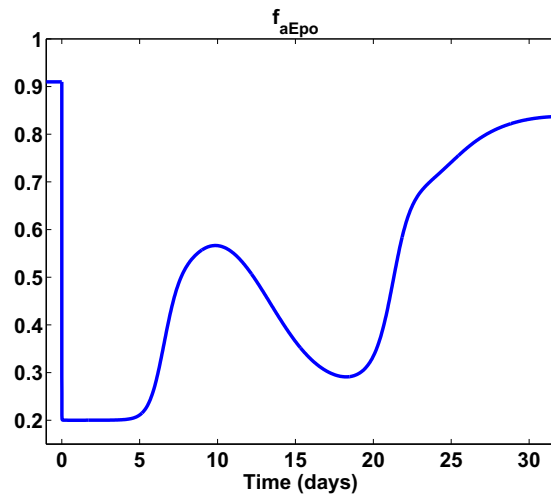


Figure 11: Anaemia simulation. Function $f_{aEpo}(Epo)$.

The above analysis enlightens two different and clear mechanisms of erythropoiesis regulation: first, inhibition of apoptosis by Epo in the early stages of the response to anaemia, and second, a more moderate regulation on the long-term of erythroid progenitor self-renewal, differentiation and apoptosis based on intracellular regulation (Erk and Fas).

Although close to experimental data, the simulated erythrocyte count (blue dash curve) does not appear to be the best fit to the data. Focusing on the nature of the anaemia, that is the consequences of phenylhydrazine use, we can obtain better results.

Phenylhydrazine is known to damage cell membrane, which results in reduced lifetime of erythrocytes following the injections. We tested this assumption with our model, assuming a mortality rate of erythrocytes $\delta = 1/30 \text{ d}^{-1}$, which means the average lifetime of an erythrocyte is reduced to 30 days under the action of phenylhydrazine. Red dash-dot curve in Figure 10 represents erythrocyte count in this case. It provides a better fit of the data, with a stronger

slope on the first days (days 1 to 5), a smaller undershoot afterward and a faster return to the equilibrium. It should be noted that the current modification of the value of δ does not alter the above analysis and conclusions, it only allows a better fit of the data. For both simulations presented in Figure 10, one feature of experimental curve is however not well approached: the undershoot in both simulations (observed around day 18) is slower, occurs later and is also smaller than the one obtained in the experiments (observed around day 14).

We confronted our model with other experimental data on phenylhydrazine-induced anaemia, presented in Crauste et al. [11]. In these experiments, haematocrit values were measured during 45 days after anaemia induction. The model used in this work does not a priori provide haematocrit, but only erythrocyte count. Haematocrit $H(t)$ is defined by

$$H(t) = \frac{vM(t)}{vM(t) + \text{Plasma volume}},$$

where $vM(t)$ represents the volume of erythrocytes in the blood. In Crauste et al. [11] we assumed that the plasma volume was not modified during the experiments and considering normal haematocrit H^* (assumed to equal 50%) and erythrocyte count M^* we obtained

$$H^* = \frac{vM^*}{vM^* + \text{Plasma volume}},$$

which provides

$$\text{Plasma volume} = \frac{1 - H^*}{H^*} vM^*.$$

Consequently, haematocrit can be deduced from the erythrocyte count,

$$H(t) = \frac{M(t)}{M(t) + (1 - H^*)M^*/H^*}.$$

This is displayed in Figure 12.

To obtain an overshoot on day 5 as presented in Figure 12, it was necessary to modify functions $f_{aEpo}(Epo)$, $p_s(E - F)$ and $a(F - E)$. In particular, the minimum value of f_{aEpo} has been dropped from 0.2 down to 0.1, see (18), functions $p_s(E - F)$ and $a(F - E)$ have been modified to have smaller variations on the relevant intervals of $F - E$. One can observe that experimental results are properly reproduced by the model, although the decrease following the peak in haematocrit values is slower in the model. Erythrocyte lifespan must be reduced from 40 days to 15 days to obtain these results, similarly to what has been done in Crauste et al. [11].

Hence, this model is able to reproduce features of a simpler model, and also leads to more insights into regulatory mechanisms of erythropoiesis.

7. Discussion

We built up a new multi-scale mathematical model of erythropoiesis taking into account several biological aspects known up to now. In particular, we

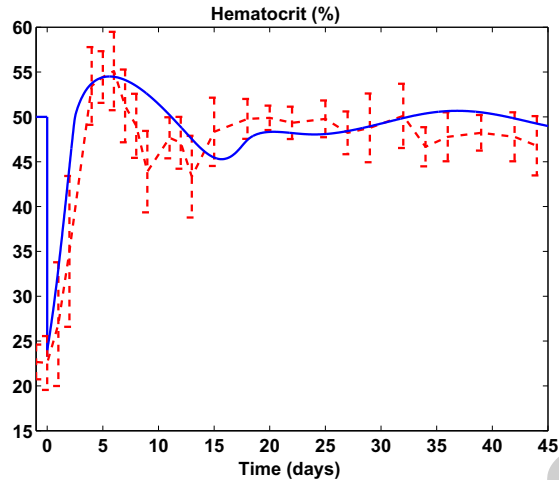


Figure 12: Anaemia simulation. Haematocrit dynamics. Blue solid line represents simulation results, red dash line represents results of experiments on induced anaemia in mice obtained in Crauste et al. [11]. Normal haematocrit is assumed to equal 50%, lifetime of erythrocytes is 15 days.

considered an intracellular network regulating cell fate, based on two proteins: Erk and Fas. These proteins, together with growth factors (erythropoietin and glucocorticoids), act on cell proliferation, and in turn the number of erythroid progenitor and of erythrocytes controls the production of growth factors and the activation of intracellular proteins. Erythropoietin was also supposed to directly inhibit progenitor apoptosis, and to contribute to intracellular proteins activation.

The resulting mathematical model was briefly analysed and numerically simulated. We focused on simulations of phenylhydrazine-induced anaemia for which parameter values were estimated. Outputs of the model were confronted with experimental data. Although most parameter values were determined through numerical simulations (due to a lack of information in the literature), we then identified two different roles of the feedback controls in response to anaemia: feedback by Epo on apoptosis (inhibition), independently of the intracellular network based on Erk and Fas, was found to be determinant in the early stage of the response, to quickly increase the number of erythrocytes, whereas feedback control through the intracellular regulatory network, introduced in Section 2, was more important later in the response, when the erythrocyte count almost reached its equilibrium value, to regulate on a long-term the response to the stress. This explained, in particular, a surprising fall in erythrocyte count although normal erythrocyte count was still not reached in Cherukuri et al data [9] (Figure 4). It must be noted, however, that Epo has a permanent influence on progenitor apoptosis.

Apart from the study of feedback functions roles and relevance, the model

brought some additional features. One deals with the apoptosis rate. The simulation provided that the apoptosis rate in mature sub-populations at the equilibrium (normal erythropoiesis) equals $a^* = 0.41 \text{ d}^{-1}$. Thus, the model suggests that in normal erythropoiesis between 40% and 50% of mature erythroid progenitors undergo apoptosis daily. Such a prediction of the model could be experimentally tested. The model also shows that in stress situations, like anaemia, the organism reacts by temporarily suppressing apoptosis that allows fast recovery of erythrocytes (Figure 9).

Regarding the model of erythropoiesis, some assumptions deserve to be commented.

All the simulations were performed under the assumption that cell cycle durations were constant, equal to one day. Although there is no evidence that cell cycles vary during response to a stress, nor that such variations could be important, this assumption appears restrictive. In particular, it is responsible in part for the delay observed in the first days of the response for the increase of the erythrocyte count. Hence, considering that cell cycles can be shortened during stress erythropoiesis could enhance the results of the proposed model, by allowing a better fit to the data, and consequently more relevance of the predicted parameters. Nevertheless, the variations of cell cycle durations could not be, to our knowledge, fitted on experimental data and would be decided in a more ad hoc way.

An other point that could potentially lead to a better model concerns the variability in Erk and Fas concentrations within a sub-population of progenitors with the same maturity. In this work we assumed that all erythroid progenitors with the same maturity had similar concentrations of Erk and Fas. Thus, our model does not take into account stochasticity in these expressions, which can play an important role in the regulation of erythropoiesis. One appropriate approach taking into account stochasticity is the individual-based modelling. This considers each cell as an independent element of the whole system and, thus, every cell can have its own properties and protein concentrations.

Let us finally comment on erythropoietin regulation. It is known that Epo levels rise due to the lack of haemoglobin. In this work we did not consider haemoglobin and we assumed that erythrocyte count alters Epo levels (thus implicitly supposing that erythrocyte count and haemoglobin are linearly dependent). Nevertheless, as shown in Cherukuri et al. [9], there is no linear dependence between haemoglobin and erythrocyte (or red blood cell) count during anaemia. This point can be relevant for the modelling of the response to anaemia. Another point is that no information is currently available about how sensitivity to Epo evolves with maturation. These aspects of Epo regulation should be investigated to improve erythropoiesis modelling.

Acknowledgements

We would like to thank Samuel Bernard, Stéphane Génieys and Laurent Pujot-Menjouet for useful remarks that allowed to improve the model presented

in this paper. We would like to express our gratitude to Dr. Mark Koury for discussions and for the experiments he implemented.

References

- [1] Ackleh, A.S., Deng, K., Cole, C.E., Tran, H.T., 2004. Existence-uniqueness and monotone approximation for an erythropoiesis age-structured model. *J. Math. Anal. Appl.* 289, 530–544.
- [2] Ackleh, A.S., Deng, K., Ito, K., Thibodeaux, J., 2006. A structured erythropoiesis model with nonlinear cell maturation velocity and hormone decay rate. *Math. Bios.* 204, 21–48, doi:10.1016/j.mbs.2006.08.004.
- [3] Adimy, M., Crauste, F., 2007. Modelling and asymptotic stability of a growth factor-dependent stem cells dynamics model with distributed delay. *Discret. Cont. Dyn. Sys. Ser. B* 8 (1), 19–38.
- [4] Al-Huniti, N.H., Widness, J.A., Schmidt, R.L., Veng-Pedersen, P., 2005. Pharmacodynamic analysis of changes in reticulocyte subtype distribution in phlebotomy-induced stress erythropoiesis. *Journal of Pharmacokinetics and Pharmacodynamics* 32, 359–376.
- [5] Banks, H.T., Cole, C.E., Schlosser, P.M., Hien, T., 2004. Modelling and optimal regulation of erythropoiesis subject to benzene intoxication. *Math. Bio. Engineering* 1(1), 15–48.
- [6] Bauer, A., Tronche, F., Wessely, O., Kellendonk, C., Reichardt, H.M., Steinlein, P., Schutz, G., Beug, H., 1999. The glucocorticoid receptor is required for stress erythropoiesis. *Genes Dev.* 13, 2996–3002.
- [7] Bélair, J., Mackey, M.C., Mahaffy, J.M., 1995. Age-structured and two-delay models for erythropoiesis. *Math. Biosci.* 128, 317–346, doi:10.1016/0025-5564(94)00078-E
- [8] Chappell, D., Tilbrook, P.A., Bittorf, T., Colley, S.M., Meyer, G.T., Klinken, S.P., 1997. Prevention of apoptosis in J2E erythroid cells by erythropoietin: Involvement of JAK2 but not MAP kinases. *Cell Death and Differentiation* 4, 105–113.
- [9] Cherukuri, S., Tripoulas, N.A., Nurko, S., Fox, P.L., 2004. Anemia and impaired stress-induced erythropoiesis in aceruloplasminemic mice. *Blood Cells, Molecules, and Diseases* 33, 346–355.
- [10] Chickarmane, V., Enver, T., Peterson, C., 2009. Computational modeling of the hematopoietic erythroid-myeloid switch reveals insights into cooperativity. *PLoS Comput. Biol.* 5, doi:10.1371/journal.pcbi.1000268.

- [11] Crauste, F., Pujo-Menjouet, L., Génieys, S., Molina, C., Gandrillon, O., 2008. Adding self-renewal in committed erythroid progenitors improves the biological relevance of a mathematical model of erythropoiesis. *J. Theor. Biol.* 250, 322–338, doi:10.1016/j.jtbi.2007.09.041.
- [12] Dazy, S., Damiola, F., Parisey, N., Beug, H., Gandrillon, O., 2003. The MEK-1/ERKs signalling pathway is differentially involved in the self-renewal of early and late avian erythroid progenitor cells. *Oncogene* 22, 9205–9216.
- [13] De Maria, R., Testa, U., Luchetti, L., Zeuner, A., Stassi, G., Pelosi, E., Riccioni, R., Felli, N., Samoggia, P., Peschle, C., 1999. Apoptotic role of Fas/Fas ligand system in the regulation of erythropoiesis. *Blood* 93, 796–803.
- [14] Demin, I., Crauste, F., Gandrillon, O., Volpert, V., 2009. A multi-scale model of erythropoiesis. *J. Biol. Dynamics* 4, 59–70.
- [15] Finch, C.A., Hanson, M.L., Donohue, D.M., 1959. Kinetics of erythropoiesis. a comparison of response to anemia induced by phenylhydrazine and by blood loss. *Am. J. Physiol.* 197, 761–764.
- [16] Fortin, P., Mackey, M.C., 1999. Periodic chronic myelogenous leukemia: Spectral analysis of blood cell counts and aetiological implications. *Brit. J. Haematol.* 104, 336–345.
- [17] Gandrillon, O., Schmidt, U., Beug, H., Samarut, J., 1999. TGF-beta cooperates with TGF-alpha to induce the self-renewal of normal erythrocytic progenitors: evidence for an autocrine mechanism. *Embo. J.* 18, 2764–2781.
- [18] Gregory, T., Yu, C., Ma, A., Orkin, S.H., Blobel, G.A., Weiss, M.J., 1999. GATA-1 and erythropoietin cooperate to promote erythroid cell survival by regulating bcl-xL expression. *Blood* 94, 87–96.
- [19] Huang, S., Guo, Y.-P., May, G., Enver, T., 2007. Bifurcation dynamics in lineage-commitment in bipotent progenitor cells. *Dev. Biol.* 305, 695–713.
- [20] Koury, M.J., Bondurant, M.C., 1990. Erythropoietin retards DNA breakdown and prevents programmed death in erythroid progenitor cells. *Science* 248, 378–381.
- [21] Kowal-Vern, A., Mazzella, F.M., Cotelingam, J.D., Shrit, M.A., Rector, J.T., Schumacher, H.R., 2000. Diagnosis and characterization of acute erythroleukemia subsets by determining the percentages of myeloblasts and proerythroblasts in 69 cases. *Am. J. Hematol.* 65, 5–13.
- [22] Liapi, C., Chrousos, G.P. Chapter 41, pp. 466–475, in Yaffe, S.J., Aranda, J.V., 1992. *Pediatric pharmacology*. 2nd ed. W.B. Saunders Company, Philadelphia.

- [23] Mackey, M.C., 1978. Unified hypothesis of the origin of aplastic anaemia and periodic hematopoiesis. *Blood* 51, 941–956.
- [24] Mackey, M.C., 1979. Dynamic hematological disorders of stem cell origin, in G. Vassileva-Popova and E. V. Jensen (Eds), *Biophysical and Biochemical Information Transfer in Recognition*. Plenum Press, New York, pp. 373–409.
- [25] Mackey, M.C., Rudnicki, R., 1994. Global stability in a delayed partial differential equation describing cellular replication. *J. Math. Biol.* 33, 89–109.
- [26] Madan, A., Lin, C., Wang, Z., Curtin, P.T., 2003. Autocrine stimulation by erythropoietin in transgenic mice results in erythroid proliferation without neoplastic transformation. *Blood Cells, Molecules and Diseases* 30, 82–89.
- [27] Mahaffy, J.M., Belair, J., Mackey, M.C., 1998. Hematopoietic model with moving boundary condition and state dependent delay: applications in erythropoiesis. *J. Theor. Biol.* 190, 135–146, doi:10.1006/jtbi.1997.0537
- [28] Mazzella, F.M., Alvares, C., Kowal-Vern, A., Schumacher, H.R., 2000. The acute erythroleukemias. *Clin. Lab. Med.* 20, 119–137.
- [29] Munugalavadla V., Kapur, R., 2005. Role of c-Kit and erythropoietin receptor in erythropoiesis. *Critical Reviews in Oncology/Hematology* 54, 63–75.
- [30] Nagata, Y., Takahashi, N., Davis, R.J., Todokoro, K., 1998. Activation of p38 MAP kinase and JNK but not ERK is required for erythropoietin-induced erythroid differentiation. *Blood* 92, 1859–1869.
- [31] Piroso, E., Erslev, A.J., Flaharty, K.K., Caro, J., 1991. Erythropoietin life span in rats with hypoplastic and hyperplastic bone marrows. *Am. J. Hematol.* 36, 105–110.
- [32] Ridley, D.M., Dawkins, F., Perlin, E., 1994. Erythropoietin: a review. *J. Natl. Med. Assoc.* 86, 129–135.
- [33] Roeder I., Glauche, I., 2006. Towards an understanding of lineage specification in hematopoietic stem cells: A mathematical model for the interaction of transcription factors GATA-1 and PU.1. *J. Theor. Biol.* 241, 852–865, doi:10.1016/j.jtbi.2006.01.021.
- [34] Rubiolo, C., Piazzolla, D., Meissl, K., Beug, H., Huber, J.C., Kolbus, A., Baccarini, M., 2006. A balance between Raf-1 and Fas expression sets the pace of erythroid differentiation. *Blood* 108, 152–159.
- [35] Sawyer, S.T., Jacobs-Helber, S.M., 2000. Unraveling distinct intracellular signals that promote survival and proliferation: study of erythropoietin, stem cell factor, and constitutive signaling in leukemic cells. *J. Hematother. Stem Cell Res.* 9, 21–29.

- [36] Spivak, J.L., Pham, T., Isaacs, M., Hankins, W.D., 1991. Erythropoietin is both a mitogen and a survival factor. *Blood* 77, 1228–1233.
- [37] Sui, X., Krantz, S.B., You, M., Zhao, Z.J., 1998. Synergistic activation of MAP kinase (ERK1/2) by erythropoietin and stem cell factor is essential for expanded erythropoiesis. *Blood* 92, 1142–1149.
- [38] Sui, X., Krantz, S.B., Zhao, Z.J., 2000. Stem cell factor and erythropoietin inhibit apoptosis of human erythroid progenitor cells through different signalling pathways. *Br. J. Haematol.* 110, 63–70.
- [39] Vainchenker, W., Dusa, A., Constantinescu, S.N., 2008. JAKs in pathologies: Role of Janus kinases in hematopoietic malignancies and immunodeficiencies. *Seminars in Cell and Developmental Biology* 19, 385–393.
- [40] Veng-Pedersen, P., Chapel, S., Schmidt, R.L., Al-Huniti, N.H., Cook, R.T., Widness, J.A., 2002. An integrated pharmacodynamic analysis of erythropoietin, reticulocyte, and hemoglobin responses in acute anemia. *Pharmaceutical Research* 19, 1630–1635.
- [41] Weissman, I.L., 2000. Stem cells: units of development, units of regeneration, and units in evolution. *Cell* 100, 157–168, doi:10.1016/S0092-8674(00)81692-X
- [42] Wichmann, H.E., Loeffler, M., 1985. *Mathematical Modeling of Cell Proliferation*. Boca Raton, FL, CRC.
- [43] Wichmann, H.E., Loeffler, M., Pantel, K., Wulff, H., 1989. A mathematical model of erythropoiesis in mice and rats. Part 2. Stimulated erythropoiesis. *Cell Tissue Kinet.* 22, 31–49.
- [44] Wulff, H., Wichmann, H.E., Loeffler, M., Pantel, K., 1989. A mathematical model of erythropoiesis in mice and rats. Part 3. Suppressed erythropoiesis. *Cell Tissue Kinet.* 22, 51–61.